



# Combined cubature Kalman and smooth variable structure filtering: A robust nonlinear estimation strategy



S.A. Gadsden<sup>a,\*</sup>, M. Al-Shabi<sup>b</sup>, I. Arasaratnam<sup>c</sup>, S.R. Habibi<sup>a</sup>

<sup>a</sup> Department of Mechanical Engineering, McMaster University, Canada

<sup>b</sup> Mechatronics Engineering Department, Philadelphia University, Jordan

<sup>c</sup> Engineering Research and Development, Ford Motor Company, Canada

## ARTICLE INFO

### Article history:

Received 1 December 2012

Received in revised form

22 August 2013

Accepted 26 August 2013

Available online 11 September 2013

### Keywords:

Cubature Kalman filter

Smooth variable structure filter

Sliding mode estimation

Nonlinear estimation

Robust filtering

## ABSTRACT

In this paper, nonlinear state estimation problems with modeling uncertainties are considered. As demonstrated recently in literature, the cubature Kalman filter (CKF) provides the closest known approximation to the Bayesian filter in the sense of preserving second-order information contained in noisy measurements under the Gaussian assumption. The smooth variable structure filter (SVSF) has also been recently introduced and has been shown to be robust to modeling uncertainties. In an effort to utilize the accuracy of the CKF and the robustness of the SVSF, the CKF and SVSF have been combined resulting in an algorithm referred to as the CK–SVSF. The robustness and accuracy of the CK–SVSF was validated by testing it on two different computer problems, namely, a target tracking problem and the estimation of the effective bulk modulus in an electrohydrostatic actuator.

© 2013 Elsevier B.V. All rights reserved.

## 1. Introduction

The term “Bayesian filtering” refers to the problem of estimating the current state of a dynamic system in an optimal and consistent fashion as noisy measurements arrive sequentially in time using Bayes’ rule. The first landmark contribution to optimal Bayesian filtering in discrete time was made by Kalman [1]. He formulated the recursive filtering solution to linear Gaussian problems using a state space model. The Kalman filter (KF) has been broadly applied to problems covering state and parameter estimation, signal processing, target tracking, fault detection and diagnosis, and even financial analysis [2,3]. The success of the KF comes from the optimality of the Kalman gain in minimizing the trace of the a posteriori state error covariance matrix [4,5].

However, the optimality of the KF does not guarantee stability and robustness.

The KF assumes that the system model is known and linear, the system noise and the measurement noise are white, and the states have initial conditions with known means and variances [6,7]. However, the previous assumptions do not always hold in real applications. If these assumptions are violated, the KF yields suboptimal results and can become unstable [8]. Furthermore, the KF is sensitive to computer precision and the complexity of computations involving matrix inversions [9]. In an effort to further increase stability, the KF has been combined with a variety of square-root algorithms, such as the Cholesky decomposition, UD-factorization, and triangularization algorithms [10–13].

These methods are based on reformulating the KF equations by using numerically stable implementations to mathematically increase the arithmetic precision of the computation [9]. Increasing the arithmetic precision reduces the effects of round-off errors, which improves the overall numerical stability of the filter. Other methods have been

\* Corresponding author. Tel.: +1 905 525 9140x21192.

E-mail addresses: [gadsden@mcmaster.ca](mailto:gadsden@mcmaster.ca), [andrew.gadsden@gmail.com](mailto:andrew.gadsden@gmail.com) (S.A. Gadsden)

proposed to reduce the effects of modeling errors [14,15]. These techniques are based on increasing the a priori covariance matrix, which increases the gain value. This approach puts more emphasis on the measurement, as opposed to the model used by the filter [6]. The effects due to assuming Gaussian noise distributions may be minimized by implementing a Gaussian sum. This method is used to approximate the non-Gaussian probability density function (PDF) by a finite number of Gaussian PDFs [16]. This approach is computationally complex due to the number of filters that are used to approximate the overall estimate [16].

In real-world situations, however, dynamic systems are nonlinear. For nonlinear systems, the posterior density that encapsulates all the information about the current state cannot be described by a finite number of summary statistics and one has to be content with an approximate filtering solution. Popular suboptimal nonlinear filters include the extended Kalman filter (EKF) [5], the unscented Kalman filter (UKF) [8], and the recently introduced cubature Kalman filter (CKF) [17,18]. Of these filters, the CKF is reportedly the most numerically stable and accurate [17]. Equally important is that the CKF does not require Jacobians and is hence applicable to a wide range of problems.

Since nonlinear Bayesian filters are suboptimal, they are robust to modeling errors to some extent. However, when a fault occurs in the system, the parameters that characterize the system can drastically change. That is, in this case, one may expect a substantial deviation of the assumed system description from the true one. Moreover, in practice, accurate information about the noise statistics is not readily available. Fortunately however, to handle modeling errors and noise uncertainties, one may use the  $H_\infty$  filter (or minimax filter) [9]. The  $H_\infty$  filter does not make any assumption about the noise and minimizes the worst case estimation error. The main disadvantage is that its performance is highly sensitive to the choice of a number of weighting functions and a user-defined performance bound. Alternatively, given upper bounds on the level of parameter or modeling uncertainties, the smooth variable structure filter (SVSF) is proved to yield extremely robust and stable results [19,20]. The EKF and UKF have been combined with the SVSF in [21]; the results show improved stability and estimation accuracy.

The key motivation for this paper is to introduce a new estimation method, referred to as the CK–SVSF, which makes use of the accuracy of the CKF and the robustness of the SVSF. The rest of the paper is structured as follows: Section 2 briefly reviews the CKF and the SVSF. In Section 3, the CK–SVSF estimation process is described. In Section 4, the CK–SVSF is applied on two different problems: a target tracking problem, and the estimation of the bulk modulus in an electrohydrostatic actuator (EHA). Section 5 concludes the paper. Note that Appendix A lists the nomenclature used in this paper.

## 2. Estimation methods

### 2.1. Cubature Kalman filter

The CKF is derived by assuming that the predictive density of the joint state–measurement variable is Gaussian. Under

this assumption, the Bayesian filter reduces to the problem of how to compute integrals in which the integrands are all of the form “nonlinear function  $\times$  Gaussian.” The CKF uses a third-degree cubature rule to numerically compute Gaussian-weighted integrals, as opposed to the sigma point set used by the UKF. The cubature rule approximates an  $n$ -dimensional Gaussian-weighted integral as follows:

$$\int_{\mathbb{R}^{n \times n}} f(x) \mathcal{N}(x; \mu, \Sigma) dx \approx \frac{1}{2^n} f(\mu + \sqrt{\Sigma} \xi_i) \quad (2.1)$$

where a square-root factor of the covariance  $\Sigma$  satisfies the relationship  $\Sigma = \sqrt{\Sigma} \sqrt{\Sigma}^T$  and the set of  $2n$  cubature points are given by

$$\xi_i = \begin{cases} \sqrt{n} e_i, & i = 1, 2, \dots, n \\ -\sqrt{n} e_{i-n}, & i = n+1, n+2, \dots, 2n \end{cases}$$

where  $e_i \in \mathbb{R}^n$  denotes the  $i$ th elementary column vector. The third-degree cubature rule is exact for polynomial integrands up to the third degree or for any odd-degree polynomial. For a detailed account of how the cubature points are derived, the reader is referred to [17]. The objective of the CKF algorithm is to recursively compute the probability  $p(x_{k+1} | z_{1:k+1}) = \mathcal{N}(\hat{x}_{k+1|k+1}, P_{k+1|k+1})$  given the posterior density  $p(x_k | z_{1:k}) = \mathcal{N}(\hat{x}_{k|k}, P_{k|k})$  at time  $k$ . Its procedural steps are described next. The initial set of cubature points  $X$  are calculated based on the previous a posteriori state estimate  $\hat{x}_{k|k}$ , the previous a posteriori state covariance  $P_{k|k}$ , and the cubature-point set  $\xi_i$  (described earlier)

$$X_{i,k|k} = \sqrt{P_{k|k}} \xi_i + \hat{x}_{k|k} \quad i = 1, 2, \dots, 2n \quad (2.2)$$

These cubature points are then propagated through the system equation, as follows:

$$X_{i,k+1|k}^* = f(X_{i,k|k}, u_k) \quad i = 1, 2, \dots, 2n \quad (2.3)$$

Next, the predicted state  $\hat{x}_{k+1|k}$  and predicted state error covariance  $P_{k+1|k}$  are calculated, respectively

$$\hat{x}_{k+1|k} = \frac{1}{2n} \sum_{i=1}^{2n} X_{i,k+1|k}^* \quad (2.4)$$

$$P_{k+1|k} = \frac{1}{2n} \sum_{i=1}^{2n} X_{i,k+1|k}^* X_{i,k+1|k}^{*T} - \hat{x}_{k+1|k} \hat{x}_{k+1|k}^T + Q_{k+1} \quad (2.5)$$

The predicted cubature points  $X_{i,k+1|k}$  are then evaluated based on the predicted state  $\hat{x}_{k+1|k}$  and predicted state error covariance  $P_{k+1|k}$

$$X_{i,k+1|k} = \sqrt{P_{k+1|k}} \xi_i + \hat{x}_{k+1|k} \quad i = 1, 2, \dots, 2n \quad (2.6)$$

The predicted cubature points  $X_{i,k+1|k}$  are then propagated through the measurements  $Z_{i,k+1|k}$ , and the corresponding predicted measurement is calculated  $\hat{z}_{k+1|k}$ , respectively as follows:

$$Z_{i,k+1|k} = h(X_{i,k+1|k}, u_{k+1}) \quad i = 1, 2, \dots, 2n \quad (2.7)$$

$$\hat{z}_{k+1|k} = \frac{1}{2n} \sum_{i=1}^{2n} Z_{i,k+1|k} \quad (2.8)$$

In order to calculate the corresponding cubature Kalman gain  $W_{k+1}$ , the innovation covariance  $P_{zz,k+1|k}$  and cross-covariance  $P_{xz,k+1|k}$  matrices need to be evaluated,

respectively as follows:

$$P_{zz,k+1|k} = \frac{1}{2n} \sum_{i=1}^{2n} Z_{i,k+1|k} Z_{i,k+1|k}^T - \hat{z}_{k+1|k} \hat{z}_{k+1|k}^T + R_{k+1} \quad (2.9)$$

$$P_{xz,k+1|k} = \frac{1}{2n} \sum_{i=1}^{2n} X_{i,k+1|k} Z_{i,k+1|k}^T - \hat{x}_{k+1|k} \hat{z}_{k+1|k}^T \quad (2.10)$$

The CKF gain may now be calculated as follows:

$$W_{k+1} = P_{xz,k+1|k} P_{zz,k+1|k}^{-1} \quad (2.11)$$

Finally, the updated states  $\hat{x}_{k+1|k+1}$  and corresponding error covariance  $P_{k+1|k+1}$  may be found

$$\hat{x}_{k+1|k+1} = \hat{x}_{k+1|k} + W_{k+1} (Z_{k+1} - \hat{z}_{k+1|k}) \quad (2.12)$$

$$P_{k+1|k+1} = P_{k+1|k} + W_{k+1} P_{zz,k+1|k} W_{k+1}^T \quad (2.13)$$

The CKF process may be summarized by the previous equations, and is repeated iteratively. For further information on the CKF and its derivation, the reader may refer to [17].

## 2.2. Smooth variable structure filter

A new form of predictor–corrector estimator based on sliding mode concepts referred to as the variable structure filter (VSF) was introduced in 2003 [22]. Essentially this method makes use of the variable structure theory and sliding mode concepts. It uses a switching gain to converge the estimates to within a boundary of the true state values (i.e., existence subspace). In 2007, the smooth variable structure filter (SVSF) was derived which makes use of a simpler and less complex gain calculation [19]. In its present form, the SVSF has been shown to be stable and robust to modeling uncertainties and noise, when given an upper bound on the level of un-modeled dynamics and noise [22–24]. The SVSF method is model based and may be applied to differentiable linear or nonlinear dynamic equations. The basic estimation concept of the SVSF is shown in Fig. 1.

The estimation process is iterative and may be summarized by the following set of equations. The predicted state estimates  $\hat{x}_{k+1|k}$  and state error covariance  $P_{k+1|k}$  are first calculated respectively as follows:

$$\hat{x}_{k+1|k} = f(\hat{x}_{k|k}, u_k) \quad (2.14)$$

$$P_{k+1|k} = F_k P_{k|k} F_k^T + Q_k \quad (2.15)$$

Note that the partial derivative of the nonlinear system function is used to create the linearized system matrix  $F_k$  as follows:

$$F_k = \left. \frac{\partial f}{\partial x} \right|_{\hat{x}_{k|k}, u_k} \quad (2.16)$$

Utilizing the predicted state estimates  $\hat{x}_{k+1|k}$ , the corresponding predicted measurements  $\hat{z}_{k+1|k}$  and measurement errors  $e_{z,k+1|k}$  may be calculated

$$\hat{z}_{k+1|k} = h(\hat{x}_{k+1|k}) \quad (2.17)$$

$$e_{z,k+1|k} = Z_{k+1} - \hat{z}_{k+1|k} \quad (2.18)$$

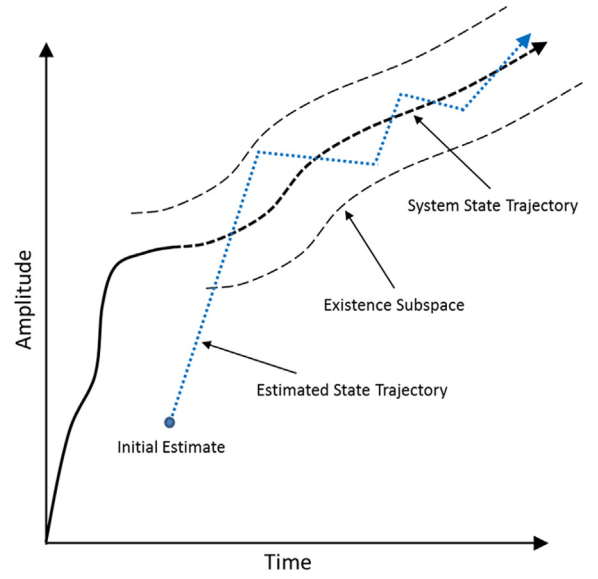


Fig. 1.

The SVSF process differs from the KF in how the gain is formulated. The SVSF gain is a function of: the a priori and the a posteriori measurement errors  $e_{z,k+1|k}$  and  $e_{z,k|k}$ ; the smoothing boundary layer widths  $\psi_i$ ; and the “SVSF” memory or convergence rate  $\gamma$ . The SVSF gain  $K_{k+1}$  is defined as follows [19,20]:

$$K_{k+1} = H_k^+ \text{diag}[(|e_{z_{k+1|k}}| + \gamma |e_{z_{k|k}}|) \circ \text{sat}(\bar{\psi}^{-1} e_{z_{k+1|k}})] \text{diag}(e_{z_{k+1|k}})^{-1} \quad (2.19)$$

where  $\circ$  signifies Schur (or element-by-element) multiplication and the superscript  $+$  refers to the pseudoinverse of a matrix. Note that the partial derivative of the nonlinear measurement function is used to create a linearized measurement matrix  $H_k$  as follows:

$$H_k = \left. \frac{\partial h}{\partial x} \right|_{\hat{x}_{k|k}, u_k} \quad (2.20)$$

The saturation function of (2.19) is defined by the following equation:

$$\text{sat}(\bar{\psi}^{-1} e_{z_{k+1|k}}) = \begin{cases} 1, & e_{z_{i,k+1|k}}/\psi_i \geq 1 \\ e_{z_{i,k+1|k}}/\psi_i, & -1 < e_{z_{i,k+1|k}}/\psi_i < 1 \\ -1, & e_{z_{i,k+1|k}}/\psi_i \leq -1 \end{cases} \quad (2.21)$$

where  $\bar{\psi}^{-1}$  is a diagonal matrix constructed from the elements of the smoothing boundary layer vector  $\psi$

$$\bar{\psi}^{-1} = \begin{bmatrix} \frac{1}{\psi_1} & 0 & 0 \\ 0 & \ddots & 0 \\ 0 & 0 & \frac{1}{\psi_m} \end{bmatrix} \quad (2.22)$$

Similar to the KF strategy, the state estimates  $\hat{x}_{k+1|k}$  and state error covariance matrix  $P_{k+1|k}$  are updated respectively as follows:

$$\hat{x}_{k+1|k+1} = \hat{x}_{k+1|k} + K_{k+1} e_{z,k+1|k} \quad (2.23)$$

$$P_{k+1|k+1} = (I - K_{k+1}H_k)P_{k+1|k}(I - K_{k+1}H_k)^T + K_{k+1}R_{k+1}K_{k+1}^T \quad (2.24)$$

Finally, the updated measurement estimate  $\hat{z}_{k+1|k+1}$  and measurement errors  $e_{z,k+1|k+1}$  are calculated, and are used in later iterations

$$\hat{z}_{k+1|k+1} = h(\hat{x}_{k+1|k+1}) \quad (2.25)$$

$$e_{z,k+1|k+1} = z_{k+1} - \hat{z}_{k+1|k+1} \quad (2.26)$$

The existence subspace shown in Figs. 1 and 2 represents the amount of uncertainties present in the estimation process, in terms of modeling errors or the presence of noise. The width of the existence space  $\beta$  is a function of the uncertain dynamics associated with the inaccuracy of the internal model of the filter as well as the measurement model, and varies with time [19]. Typically this value is not exactly known but an upper bound may be selected

based on a priori knowledge. Once within the existence boundary subspace, the estimated states are forced (by the SVSF gain) to switch back and forth along the true state trajectory. High-frequency switching caused by the SVSF gain is referred to as chattering, and in most cases, is undesirable for obtaining accurate estimates [19]. However, the effects of chattering may be minimized by the introduction of a smoothing boundary layer  $\psi$ . The selection of the smoothing boundary layer width reflects the level of uncertainties in the filter and the disturbances (i.e., system and measurement noise, and un-modeled dynamics).

The effect of the smoothing boundary layer is shown in Fig. 2. When it is defined larger than the existence subspace boundary, the estimated state trajectory is smoothed. However, when the smoothing term is too small, chattering remains due to the uncertainties being underestimated.

### 3. CK-SVSF estimation method

The SVSF provides an estimation process that is sub-optimal albeit robust and stable. It is hence beneficial to be able to combine the accurate performances of the CKF with the stability of the SVSF. A recent development, as described in [20,25], provides a methodology for calculating a variable smoothing boundary layer  $\psi_{k+1}$ .

The partial derivative of the a posteriori covariance (trace) with respect to the smoothing boundary layer term  $\psi_{k+1}$  is the basis for obtaining a time-varying strategy for the specification of  $\psi_{k+1}$ . In linear systems, this smoothing boundary layer yields an optimal gain (exactly the KF) [20]. Previous forms of the SVSF included a vector form of  $\psi$ , which had a single smoothing boundary layer term for each corresponding measurement error [19]. Essentially, the boundary layer terms were independent of each other such that the measurement errors would not mix when calculating the corresponding gain, leading to reduced estimation accuracy. In an effort to obtain a smoothing boundary layer equation that yielded more accurate state estimates, a full smoothing boundary layer matrix was proposed in [20,25]. Hence, considering the following smoothing boundary layer form:

$$\psi = \begin{bmatrix} \psi_{11} & \psi_{12} & \cdots & \psi_{1m} \\ \psi_{12} & \psi_{22} & \cdots & \psi_{2m} \\ \vdots & \vdots & \ddots & \vdots \\ \psi_{m1} & \psi_{m2} & \cdots & \psi_{mm} \end{bmatrix} \quad (3.1)$$

This definition includes terms that relate one smoothing boundary layer to another (i.e., off-diagonal terms). To solve the time-varying smoothing boundary layer based on (3.1), the following in conjunction with (2.24) is considered:

$$\frac{\partial(\text{trace}[P_{k+1|k+1}])}{\partial\psi} = 0 \quad (3.2)$$

As described in [26], a solution for the smoothing boundary layer from (3.2) is defined as follows:

$$\psi_{k+1} = (\bar{A}^{-1}H_kP_{k+1|k}H_k^T S_{k+1}^{-1})^{-1} \quad (3.3)$$

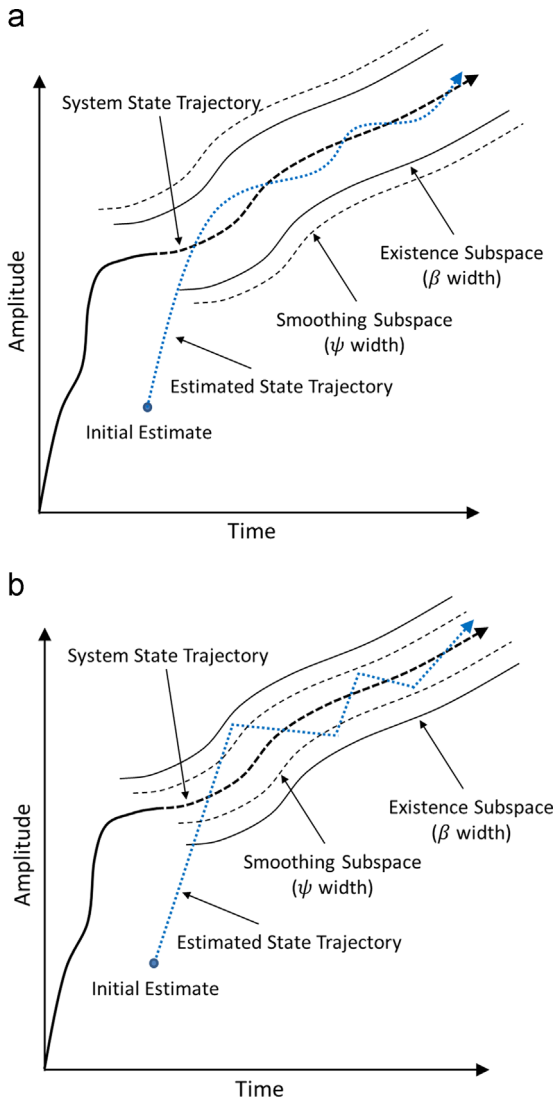


Fig. 2.

where  $S_{k+1}$  and  $A$  are defined respectively by

$$S_{k+1} = H_k P_{k+1} H_k^T + R_{k+1} \quad (3.4)$$

$$A = (|e_{z_{k+1}k}| + \gamma |e_{z_{k+1}k}|) \quad (3.5)$$

Note that in (3.3),  $\bar{A}$  refers to forming a diagonal matrix of elements consisting of  $A$ . The CKF and SVSF strategies will be combined using this smoothing boundary layer calculation. Considering the following sets of figures to help describe the overall implementation of the CK–SVSF strategy.

Fig. 3 illustrates the case when the constant smoothing boundary layer width used by the SVSF is defined larger than the time-varying smoothing boundary layer (i.e., a conservative choice) calculated by (3.3). The difference between the constant and upper layers leads to a reduction in estimation accuracy for the SVSF. Essentially, in this case, the CKF gain should be used to obtain the best result.

Fig. 4 illustrates the case when the time-varying smoothing boundary layer is calculated to exist beyond the constant smoothing boundary layer. This typically occurs when there is modeling uncertainty (which leads to a reduction in estimation accuracy) that exceed the limits of a constant smoothing boundary layer. The limits are set by the width of the existence subspace, which was discussed earlier. In a situation defined by Fig. 4 when  $\psi_{vbl} \geq \psi_{lim}$ , to ensure a stable estimate, the SVSF gain (2.19) should be used to update the state estimates. The smoothing boundary layer widths calculated by (3.3) are saturated at the constant values. This ensures a stable estimate, as defined by the proof of stability for the SVSF [19]. Furthermore, to improve the SVSF results (i.e., without the use of (3.3)), the averaged smoothing boundary layers (for the well-defined system) can be used to set the constant boundary layer widths. Doing so provides a well-tuned existence subspace that yields more accurate estimates.

Essentially, in a well-defined case, the gain used to correct the estimate is calculated by the CKF. When the smoothing boundary layer calculated by (3.3) goes beyond

the defined constant value, the smoothing boundary layer width requires saturation (at the constant value). This process effectively combines the CKF and SVSF estimation methods and creates a new estimation strategy referred to as the CK–SVSF.

For implementation, the CK–SVSF equations are summarized. Essentially, the CKF equations are used to predict the state estimates and state error covariance matrix. At this point, the time-varying smoothing boundary layer is calculated and compared with a fixed, conservative value. If the boundary layer value is smaller than the fixed value, then the CKF gain should be used to update the state estimates and state error covariance matrix. However, if the boundary layer value is calculated to exist beyond the conservative value, then the SVSF gain should be implemented. For completeness, the equations are provided in Appendix B.

#### 4. Computer experiments

In this section, the CK–SVSF is applied on two different problems: a nonlinear target tracking scenario, and the estimation of the bulk modulus parameter in an electrohydrostatic actuator (EHA). The purpose of the simulations is to demonstrate that the CK–SVSF method provides an accurate and stable estimation process when compared with the standard CKF and SVSF.

##### 4.1. Nonlinear target tracking

The nonlinear estimation problem consists of tracking a target (i.e., aircraft) with nonlinear range and bearing measurements from a sensor (i.e., radar) located at the origin. The system is represented by four states (target position and velocity, both in the  $x$ - and  $y$ -directions respectively). Uncertainty is added to the system by the lack of knowledge of the true target turn rate  $\omega$ . The nonlinear system  $x_{k+1}$  and measurements  $z_{k+1}$  are defined

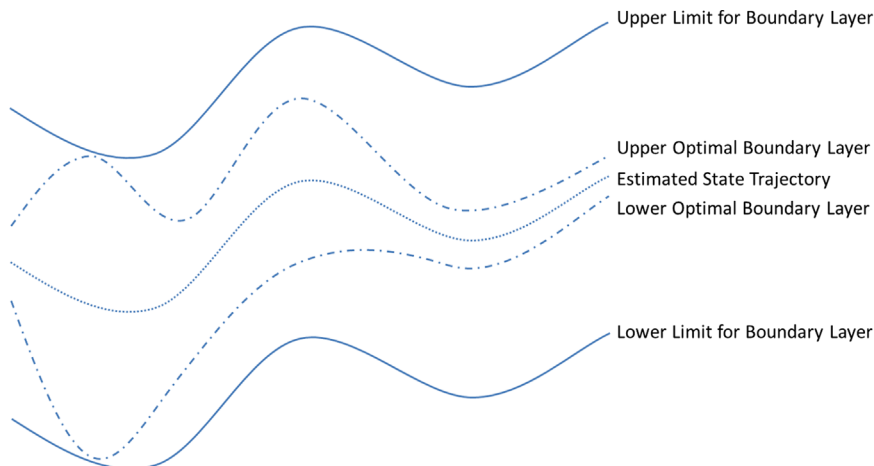


Fig. 3.

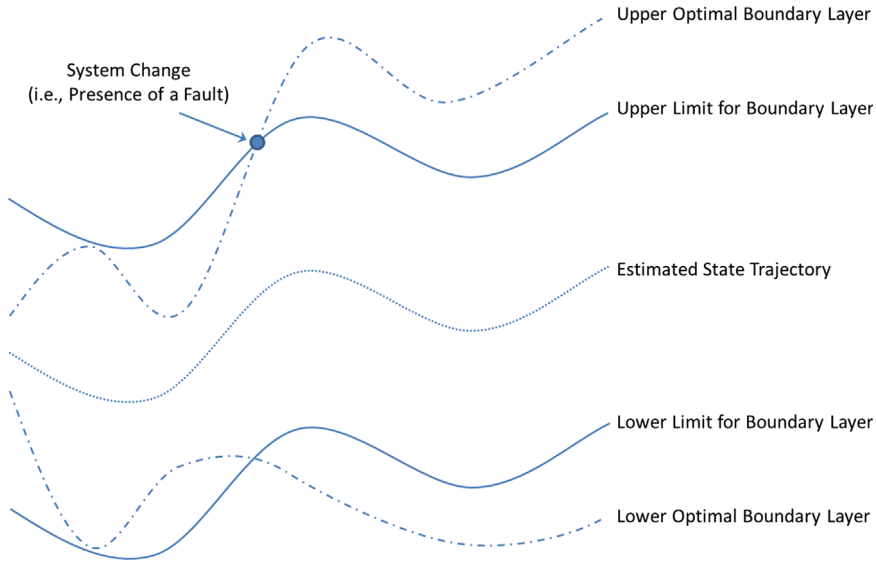


Fig. 4.

as follows [2]:

$$x_{k+1} = \begin{bmatrix} 1 & \frac{\sin(\omega T)}{\omega} & 0 & \frac{-(1-\cos(\omega T))}{\omega} \\ 0 & \cos(\omega T) & 0 & -\sin(\omega T) \\ 0 & \frac{-(1-\cos(\omega T))}{\omega} & 1 & \frac{\sin(\omega T)}{\omega} \\ 0 & \sin(\omega T) & 0 & \cos(\omega T) \end{bmatrix} x_k + w_k \quad (4.1)$$

$$z_{k+1} = \begin{bmatrix} \sqrt{x_{1,k+1}^2 + x_{3,k+1}^2} \\ \tan^{-1}\left(\frac{x_{3,k+1}}{x_{1,k+1}}\right) \\ \sqrt{x_{2,k+1}^2 + x_{4,k+1}^2} \\ \tan^{-1}\left(\frac{x_{4,k+1}}{x_{2,k+1}}\right) \end{bmatrix} + v_{k+1} \quad (4.2)$$

The measurements corresponding to (4.1) consist of the target's range, bearing, resultant speed, and resultant bearing speed. The initial state estimates were defined based on a random distribution of the true initial state values and the initial state error covariance matrix. The system noise and the measurement noise were derived based on their covariance matrices, respectively as follows [2,7]:

$$Q = \begin{bmatrix} q_1 M & \text{zeros}(2, 2) \\ \text{zeros}(2, 2) & q_2 M \end{bmatrix} \quad (4.3)$$

$$R = \text{diag}([\sigma_r^2 \quad \sigma_\theta^2]) \quad (4.4)$$

where the following are defined [2,7]:

$$M = \begin{bmatrix} \frac{T^3}{3} & \frac{T^2}{2} \\ \frac{T^2}{2} & T \end{bmatrix} \quad (4.5)$$

$$\sigma_r = 10 \quad (4.6)$$

$$\sigma_\theta = 0.25 \frac{\pi}{180} \quad (4.7)$$

$$q_1 = 0.001 \quad (4.8)$$

$$q_2 = 0.01 \frac{\pi}{180} \quad (4.9)$$

The initial state error covariance was defined as follows:

$$P_{0|0} = \text{diag}([100 \quad 10 \quad 100 \quad 10]) \quad (4.10)$$

For the standalone SVSF estimation process, the constant smoothing boundary layer widths were defined as  $\psi = [5 \quad 15 \quad 5 \quad 10 \quad 1.5]^T$ , and the SVSF “memory” or convergence rate was set to  $\gamma = 0.1$ . These parameters were tuned based on some knowledge of the uncertainties (i.e., magnitude of noise) and with the goal of decreasing the estimation error. In this problem, two different cases were studied. The first case involved the target turning once. The second case involved the target turning twice, introducing further uncertainty in the estimation process. Also, note that the sample rate  $T$  of the radar was 1 s. The target tracking results are shown in the following sets of figures. The EKF, CKF, SVSF, and the new CK–SVSF methods were applied.

The RMSE results of running the simulation are listed in two tables (for each case respectively), shown in Appendix C. As shown in these tables, the new CK–SVSF method performed the best in terms of accuracy (i.e., RMSE). The SVSF switching “effect” is shown clearly in Figs. 5 and 6. The switching, inherent to the SVSF gain, ensures that the estimation process is robust and stable. However, note that the SVSF yielded the worst turn rate estimate for both cases, but estimated the position and velocity of the target very well. As demonstrated in Fig. 6, the EKF and CKF methods were unable to provide a good estimate of the target after the second turn. Bounding the CKF to within a region of the measurements by use of the SVSF further increased the stability and the performance as shown by the results of the CK–SVSF method. The strategy effectively combined the accuracy of the CKF and the stability of the SVSF.

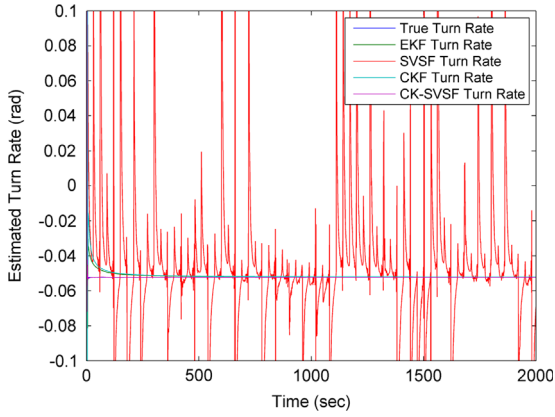


Fig. 5.

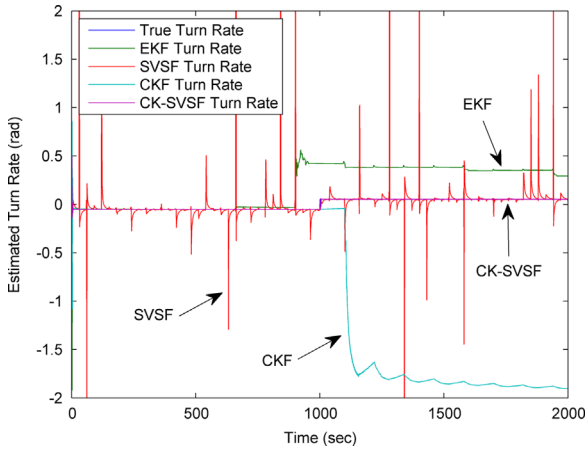


Fig. 6.

#### 4.2. Estimation of the effective bulk modulus in an EHA

In this experiment, an electrohydrostatic actuator (EHA) is simulated based on an actual prototype built for experimentation [19,23]. The purpose of this simulation is to demonstrate that the combined estimation process (CK–SVSF) yields a very accurate estimate, without negatively impacting its stability to modeling errors or uncertainties.

The EHA is a third order (typically linear) system with state variables related to its position, velocity, and acceleration. It is assumed that all three states have measurements associated with them (i.e., full measurement matrix). The input to the system is a random normal distribution with magnitude 1. The sample time  $T$  of the system is 0.001 s. The entire EHA system description may be found in [19]. The open-loop transfer function of the system is defined as follows:

$$\frac{x(s)}{u(s)} = \frac{2D_p\beta_e A_E / MV_0}{s^3 + ((B_E/M) + (L/V_0)\beta_e)s^2 + (2\beta_e A_E^2 / MV_0)s} \quad (4.11)$$

For the purpose of this paper, three states (kinematic information) and one parameter (the effective bulk

**Table 1**  
EHA parameter values.

Term	Physical significance	EHA model value
$A_E$	Piston area	$3.37 \times 10^{-4} \text{ m}^2$
$B_E$	Load friction	1260 Ns/m
$D_p$	Pump displacement	$6.69 \times 10^{-3} \text{ m}^3/\text{rad}$
$L$	Leakage coefficient	$5 \times 10^{-12} \text{ m}^3/\text{s Pa}$
$M$	Load mass	20 kg
$V_0$	Chamber volume	$8.5 \times 10^{-5} \text{ m}^3$
$\beta_e$	Effective bulk modulus	$2.1 \times 10^8 \text{ Pa}$

modulus) will be estimated. The estimation of the parameter creates a nonlinear estimation problem. The system model equations are defined as follows:

$$x_{1,k+1} = x_{1,k} + Tx_{2,k} \quad (4.12)$$

$$x_{2,k+1} = x_{2,k} + Tx_{3,k} \quad (4.13)$$

$$x_{3,k+1} = (1 - T\varphi_3 - T\varphi_2 x_{4,k})x_{3,k} - T\varphi_1 x_{2,k} + G_E T x_{4,k} u_k \quad (4.14)$$

$$x_{4,k+1} = x_{4,k} \quad (4.15)$$

where the following are defined:

$$G_E = \frac{2D_p A_E}{MV_0} \quad (4.16)$$

$$\varphi_1 = \frac{2A_E^2}{MV_0} \quad (4.17)$$

$$\varphi_2 = \frac{L}{V_0} \quad (4.18)$$

$$\varphi_3 = \frac{B_E}{M} \quad (4.19)$$

The EHA parameter values used in this computer experiment are given in Table 1.

The initial state values are set to zero. The initial true bulk modulus is set to  $x_{4,0} = 2.1 \times 10^8 \text{ Pa}$ , whereas the corresponding initial estimate is  $\hat{x}_{4,0} = 1.5 \times 10^8 \text{ Pa}$ .

Half-way through the simulation the true effective bulk modulus is changed to  $1.5 \times 10^8 \text{ Pa}$ . The system and measurement noises are defined with maximum amplitude corresponding to  $W_{max} = [0.0001 \ 0.001 \ 0.1]^T$  and  $V_{max} = [0.0001 \ 0.001 \ 0.1]^T$  and are considered to be Gaussian. The initial state error covariance  $P_{0|0}$ , system noise covariance  $Q$ , and measurement noise covariance  $R$  are defined respectively as follows:

$$P_{0|0} = 10Q \quad (4.20)$$

$$Q = 5W_{max}W_{max}^T \quad (4.21)$$

$$R = 5V_{max}V_{max}^T \quad (4.22)$$

For the SVSF estimation process, the “memory” or convergence rate was set to  $\gamma = 0.1$ , and the smoothing boundary layer widths were defined as  $\psi = 5V_{max}$ . These parameters were set based on the level of noise and modeling uncertainty, with the goal of decreasing the estimation error. The main results of applying the EKF, CKF, SVSF, and the CK–SVSF on the EHA problem are shown in the following sets of figures. Fig. 7 shows the

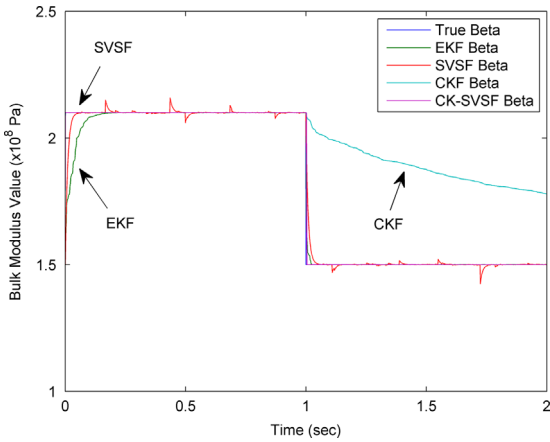


Fig. 7.

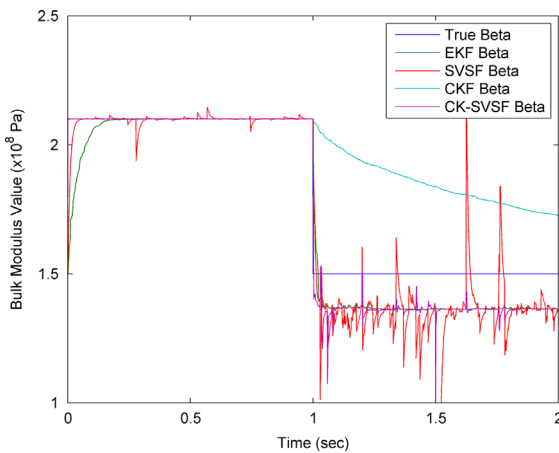


Fig. 8.

effective bulk modulus estimates provided by all of the strategies. Initially, both the CKF and CK–SVSF responded the fastest, followed by the SVSF and the EKF. The CKF responded well because the initial covariance matrix was well-defined. However, when the bulk modulus changed half-way through the simulation, the CKF was unable to estimate the parameter very well. The CK–SVSF worked the best in this case. Note that the CK–SVSF estimate was nearly on-top of the true value, thus it is difficult to distinguish in Fig. 7 (and its label was omitted).

As shown in the first table of Appendix D, the CK–SVSF provides the best overall result in terms of estimation accuracy and rate of convergence. In the next case, the robustness of the combined method is shown when modeling errors are introduced into the experiment. The next figure shows the estimates of the parameter, but with the addition of modeling errors. This was accomplished by adding 10% uncertainty to the mass value used by the filters.

The RMSE results for this case are shown in the second table of Appendix D. The effect of changing the mass used by

the filters in the estimation process is clearly shown at one second. The “switching” or chattering characteristics of the SVSF gain are clearly present, as shown in Fig. 8. The combined methodology provided the best parameter estimate. However, the SVSF yielded the best state estimates. In this example, the system is only mildly nonlinear, and the measurement matrix is linear. “Mildly nonlinear” refers to a system that may be approximated by a piece-wise linear system as opposed to a higher-order function. As such, it may be sufficient to represent the nonlinearities using a first-order Taylor series approximation, as opposed to the statistical approximation performed by the CKF.

## 5. Conclusions

This paper introduced a new estimation method referred to as the CK–SVSF, which utilizes the accuracy of the CKF and the stability of the SVSF. The combined method may be applied to linear or nonlinear systems which may be affected by uncertainties. A nonlinear target tracking problem was used to demonstrate and compare the accuracy and robustness of the new filter with their standalone estimation strategies. In addition, a mechatronic system was used to study further and compare the combined method with other popular methods. It is recommended that this method be applied on the control of mechanical or electrical systems where one may be concerned with an accurate and robust estimation strategy.

Table A1

List of nomenclature.

Parameter	Definition
$x$	State vector or values
$z$	Measurement (system output) vector or values
$w$	System noise vector
$v$	Measurement noise vector
$F$	Linear system transition matrix
$H$	Linear measurement (output) matrix
$K$	SVSF gain matrix
$P$	State error covariance matrix
$P_{xz}$	Covariance matrix between $x$ and $z$
$P_{zz}$	Covariance matrix between $z$ and $z$
$Q$	System noise covariance matrix
$R$	Measurement noise covariance matrix
$S$	Innovation (measurement error) covariance matrix
$W$	CKF update weight or gain
$e_z$	Measurement (output) error vector
$\xi$	Array of cubature points
$\mathcal{N}(\mu, \Sigma)$	Normal distribution with mean $\mu$ and variance $\Sigma$
$E[a]$	Expectation of some vector or matrix $a$
$\gamma$	SVSF “memory” or convergence rate
$\psi$	SVSF smoothing boundary layer
$\text{diag}[a]$ or $\bar{a}$	Diagonal of some vector or matrix $a$
$\text{sat}()$	Saturation function
$ a $	Absolute value of $a$
$T$	Transpose of a vector (superscript) or sample rate
$\circ$	Denotes a Schur product
$\sim$	Denotes error or difference
$\hat{\cdot}$	Estimated vector or values

## Appendices

### A. Nomenclature

See Appendix [Table A1](#).

### B. Summary of the CK–SVSF estimation process

The following is a pseudocode for the CK–SVSF estimation process.

1. *Initialization stage*:
  - a. Initialize state estimates (e.g., zeros).
  - b. Initialize state error covariance matrix (e.g., typically a diagonal matrix).
  - c. Initialize measurement errors (e.g., zeros).
2. *Prediction stage*:
  - a. Predict state estimates using cubature rules.
  - b. Predict state error covariance matrix using cubature rules.
  - c. Predict measurements using cubature rules.

- d. Predict measurement error covariance matrix using cubature rules.
  - e. Calculate a priori measurement error.
3. *Smoothing boundary layer stage*:
    - a. Calculate the time-varying smoothing boundary layer.
    - b. Compare the calculated value (from 3a) with the fixed value.
      - i. If 3a value is greater than fixed value, proceed to 4a.
      - ii. If 3a value is less than or equal to fixed value, proceed to 4b.
  4. *Update stage*:
    - a. Calculate the SVSF gain.
    - b. Calculate the CKF gain.
    - c. Update the state estimate using the gain.
    - d. Update the state error covariance matrix.
    - e. Calculate the a posteriori measurement error.

The CK–SVSF estimation process is iterative, and is summarized above. Note that for the linear systems case,

**Table C1**

RMSE results: single-turn maneuver.

Filter	x-Position (m)	x-Vel. (m/s)	y-Pos. (m)	y-Vel. (m/s)	Bearing (rad)
EKF	11.53	11.64	15.46	9.39	0.044
SVSF	9.33	7.11	15.48	1.53	0.264
CKF	10.61	13.22	15.65	12.79	0.036
CK–SVSF	9.26	6.73	15.45	0.33	0.012

**Table C2**

RMSE results: two-turn maneuver.

Filter	x-Position (m)	x-Vel. (m/s)	y-Pos. (m)	y-Vel. (m/s)	Bearing (rad)
EKF	1490	852	1685	1080	0.255
SVSF	9.37	7.12	15.78	3.10	3.101
CKF	2642	3680	2974	3831	1.254
CK–SVSF	9.29	6.79	15.75	0.55	0.013

**Table D1**

RMSE results: normal case.

Filter	Position (m)	Velocity (m/s)	Accel. (m/s <sup>2</sup> )	Bulk modulus (Pa)
EKF	$2.92 \times 10^{-4}$	$6.07 \times 10^{-2}$	1.07	$5.13 \times 10^{-2}$
SVSF	$5.03 \times 10^{-5}$	$3.48 \times 10^{-3}$	0.13	$4.32 \times 10^{-2}$
CKF	$1.23 \times 10^{-3}$	$2.43 \times 10^{-1}$	4.11	$2.78 \times 10^{-1}$
CK–SVSF	$2.19 \times 10^{-5}$	$1.99 \times 10^{-3}$	0.68	$2.69 \times 10^{-2}$

**Table D2**

RMSE results: modeling uncertainty case.

Filter	Position (m)	Velocity (m/s)	Accel. (m/s <sup>2</sup> )	Bulk modulus (Pa)
EKF	$1.96 \times 10^{-4}$	$8.52 \times 10^{-2}$	1.37	$1.14 \times 10^{-1}$
SVSF	$4.76 \times 10^{-5}$	$3.48 \times 10^{-3}$	0.13	$2.70 \times 10^{-1}$
CKF	$7.56 \times 10^{-4}$	$3.31 \times 10^{-1}$	5.16	$2.59 \times 10^{-1}$
CK–SVSF	$5.07 \times 10^{-5}$	$1.91 \times 10^{-2}$	0.64	$1.04 \times 10^{-1}$

the KF has been combined with the SVSF by utilizing the calculated smoothing boundary layer [26].

### C. Nonlinear target tracking results

See Appendix Tables C1 and C2.

### D. Estimation of the effective bulk modulus in an EHA results

See Appendix Tables D1 and D2.

## References

- [1] R.E. Kalman, A new approach to linear filtering and prediction problems, *Journal of Basic Engineering*, Transactions of ASME 82 (1960) 35–45.
- [2] B. Ristic, S. Arulampalam, N. Gordon, *Beyond the Kalman Filter: Particle Filters for Tracking Applications*, Artech House, Boston, 2004.
- [3] S. Haykin, *Kalman Filtering and Neural Networks*, John Wiley and Sons, Inc., New York, U.S.A., 2001.
- [4] T. Kailath, *Linear Systems*, Prentice Hall, U.S.A., 1980.
- [5] A. Gelb, *Applied Optimal Estimation*, MIT Press, Cambridge, MA, 1974.
- [6] D. Simon, *Optimal State Estimation: Kalman, H-Infinity, and Non-linear Approaches*, Wiley-Interscience, 2006.
- [7] Y. Bar-Shalom, X. Rong Li, T. Kirubarajan, *Estimation with Applications to Tracking and Navigation*, John Wiley and Sons, Inc., New York, 2001.
- [8] S.J. Julier, J.K. Uhlmann, H.F. Durrant-Whyte, A new method for non-linear transformation of means and covariances in filters and estimators, *IEEE Transactions on Automatic Control* 45 (2000) 472–482.
- [9] M.S. Grewal, A.P. Andrews, *Kalman Filtering: Theory and Practice Using MATLAB*, 3rd ed. John Wiley and Sons, Inc., New York, 2008.
- [10] P. Kaminski, A. Bryson, S. Schmidt, Discrete square root filtering: a survey of current techniques, *IEEE Transactions on Automatic Control* 16 (6) (1971) 727–736.
- [11] S. Hammarling, A Survey of Numerical Aspects of Plane Rotations, Middlesex Polytechnic, Mathematics 1749-9097, 1977.
- [12] H. Wang, R. Gregory, On the reduction of an arbitrary real square matrix to tridiagonal form, *Mathematics of Computation* 18 (87) (1964) 501–505.
- [13] J. Chandrasekar, I.S. Kim, D.S. Bernstein, A.J. Ridley, Cholesky-based reduced-rank Kalman filtering, in: *Proceedings of American Control Conference (ACC)*, 2008, pp. 3987–3992.
- [14] L. Xie, C. Soh, C.E. Souza, Robust Kalman filtering for uncertain discrete-time systems, *IEEE Transactions on Automatic Control* 39 (6) (1994) 1310–1314.
- [15] X. Zhu, Y.C. Soh, L. Xie, Design and analysis of discrete-time robust Kalman filters, *Automatic* 38 (6) (2002) 1069–1077.
- [16] B. Berndt, R. Evans, K. Williams, *Gauss and Jacobi Sums*, John Wiley & Sons, Inc., New York, U.S.A., 1998.
- [17] I. Arasaratnam, S. Haykin, Cubature Kalman filters, *IEEE Transactions on Automatic Control* 54 (6) (2009) 1254–1269.
- [18] D. Macagnano, G. De Abreu, Adaptive gating for multitarget tracking with Gaussian mixture filters, *IEEE Transactions on Signal Processing* 60 (3) (2012) 1533–1538.
- [19] S.R. Habibi, The smooth variable structure filter, *Proceedings of the IEEE* 95 (5) (2007) 1026–1059.
- [20] S.A., Gadsden Smooth Variable Structure Filtering: Theory and Applications (Ph.D. thesis), Department of Mechanical Engineering, McMaster University, Hamilton, Ontario, 2011.
- [21] M. Al-Shabi, S.A. Gadsden, S.R. Habibi, Kalman filtering strategies utilizing the chattering effects of the smooth variable structure filter, *Signal Processing* 93 (2) (2013) 420–431.
- [22] S.R. Habibi, R. Burton, The variable structure filter, *Journal of Dynamic Systems, Measurement, and Control (ASME)* 125 (2003) 287–293.
- [23] S.R. Habibi, R. Burton, Parameter identification for a high performance hydrostatic actuation system using the variable structure filter concept, *ASME Journal of Dynamic Systems, Measurement, and Control* 129 (2) (2007) 229–235.
- [24] S.A. Gadsden, Y. Song, S.R. Habibi, Novel model-based estimators for the purposes of fault detection and diagnosis, *IEEE/ASME Transactions on Mechatronics* 18 (4) (2013) 1237–1249.
- [25] S.A., Gadsden, M., El Sayed, S.R., Habibi, Derivation of an optimal boundary layer width for the smooth variable structure filter, in: *Proceedings of American Control Conference*, San Francisco, CA, USA, 2011.
- [26] S.A. Gadsden, S.R. Habibi, A new robust filtering strategy for linear systems, *ASME Journal of Dynamic Systems, Measurements and Control* 135 (1) (2013) 014503-1–014503-9.